A Systematic Study of the Vibrational Free Energies of Polypeptides in Folded and Random States

Buyong Ma,* Chung-Jung Tsai,† and Ruth Nussinov†‡

*Laboratory of Experimental and Computational Biology and †Intramural Research Support Program, SAIC, Laboratory of Experimental and Computational Biology, NCI–FCRDC, Bldg 469, Room 151, Frederick, MD 21702 USA; and ‡Sackler Institute of Molecular Medicine, Sackler Faculty of Medicine, Department of Human Genetics and Molecular Medicine, Tel Aviv University, Tel Aviv 69978, Israel

ABSTRACT Molecular vibrations, especially low frequency motions, may be used as an indication of the rigidity or the flatness of the protein folding energy landscape. We have studied the vibrational properties of native folded as well as random coil structures of more than 60 polypeptides. The picture we obtain allows us to perceive how and why the energy landscape progressively rigidifies while still allowing potential flexibility. Compared with random coil structures, both α-helices and β-hairpins are vibrationally more flexible. The vibrational properties of loop structures are similar to those of the corresponding random coil structures. Inclusion of an α-helix tends to rigidify peptides and so-called building blocks of the structure, whereas the addition of a β-structure has less effect. When small building blocks coalesce to form larger domains, the protein rigidifies. However, some folded native conformations are still found to be vibrationally more flexible than random coil structures, for example, β_2-microglobulin and the SH3 domain. Vibrational free energy contributes significantly to the thermodynamics of protein folding and affects the distribution of the conformational substates. We found a weak correlation between the vibrational folding energy and the protein size, consistent with both previous experimental estimates and theoretical partition of the heat capacity change in protein folding.

INTRODUCTION

The funnel shape energy landscape theory has been successfully used to describe the folding and binding behavior in proteins. The energy landscape in protein folding has been depicted in terms of hills, corresponding to high energy conformations, and valleys, having more favorable conformations than those in their energy-landscape vicinity. Around the bottom of the valley there is a population of conformations. If the landscape is smooth, the native protein may be expected to have small fluctuations, with only small changes in the conformations. However, if the energy landscape is rugged, the ensemble of structures would include conformations which may be quite different, depending on the extent of the ruggedness. The energy landscape theory has elegantly shown a way out of the long-standing baffling Levinthal paradox. The old view of protein folding implies a rigid and unique structure of the folded protein. However, the new theory, along with the recent experimental evidence, has indicated that folded proteins can be flexible, with many conformational substates. The existence of conformational substates has important biological implications. The properties of a protein are decided not only by the static folded three-dimensional structure, but also by the distribution of its conformational substates. In particular, the function of the protein and its properties are derived from the redistributions of the populations under different environments. That is, protein function derives from a dynamic energy landscape. Hence, the protein folding energy landscape is not a mere abstract concept; it is also a powerful way to relate the static, dynamic, and biological properties of a protein (Tsai et al., 1999; Kumar et al. 2000a).

Vibrational free energy contributes substantially to the thermodynamics of protein folding and binding. The stability of a native protein is a delicate balance between the enthalpic and entropic contributions of the polypeptide chain and the surrounding solvent. The most significant contributions derive from the conformational degrees of freedom of the chain, its vibrational modes, and the hydration of the chemical groups. Sturtevant (1977) and Kanehisa and Ikegami (1977) pointed out that changes in the frequency of internal vibrational modes also contribute to the heat capacity change. The unfolded chain was proposed to have more soft (low frequency) modes than the native protein, and a larger vibrational heat capacity. For two decades, this suggestion has been accepted without question, and the vibrational contributions to protein folding were either ignored or simply estimated, mainly by empirical models developed by Sturtevant (1977). Yet the notion that the unfolded chain has more soft (low frequency) modes than the native protein is not fully consistent with the new view of protein folding energy landscape. If the energy landscape is rugged, some native proteins may have more vibrational states. Hagler et al. (1979) first investigated the stability of α-helices in short peptides. They found that an α-helix could be favored by vibrational entropy. Tidor and Karplus (1994) studied the dimerization of insulin and found favorable vibrational entropy for the dimerization as

Received for publication 21 March 2000 and in final form 27 June 2000.

Address reprint requests to R. Nussinov, NCI–FCRF Bldg. 469, Room 151, Frederick, MD 21702. Tel.: 301-846-5579; Fax: 301-846-5598; E-mail: ruthn@ncifcrf.gov.

0006-3495/00/11/2739/15 $2.00

well. Recently, we (Ma and Nussinov, 1999) have found that β-hairpin formation in a peptide also has a favorable vibrational entropy.

The assumption that upon binding flexibility is uniformly restricted conflicts with emerging data showing that in molecular complexes, motion can increase, decrease, or remain unchanged (Zidek et al., 1999; Lee et al., 2000). It was found that the stability constants for individual residues do not exhibit the same change in magnitude upon binding (Todd and Freire, 1999). Experimental investigations of the entropic contributions from the dynamics at specific positions in a complex suggest that an increase in motion can dominate the free energy of association in certain cases. Recently, two important experimental results regarding the entropic contributions to protein binding have been published (Zidek et al., 1999; Lee et al., 2000). In the calmodulin-peptide case, Lee et al. (2000) have observed that the dynamics of side chains are significantly perturbed, indicating an extensive enthalpy/entropy exchange during the formation of a protein-protein interface. Interestingly, Zidek et al. (1999) have shown an increased protein backbone conformational entropy upon hydrophobic ligand binding. Here, we investigate changes in vibrational entropy during protein folding, a process postulated to be similar to protein-protein binding.

A study of the vibrational change during the folding process may also have implications for the protein folding energy landscape. The outline of the protein energy landscape is frequently inferred from molecular dynamics simulations using either on-lattice or off-lattice models (Lazaridis and Karplus, 1997; Bozko and Brooks, 1995; Troyer and Cohen, 1995; Kitao et al., 1998). Here, we depict the protein folding energy landscape by studying the vibrational properties of proteins in both the folded and the unfolded states. The general theory underlying this approach is that flexible proteins have more available vibrational states, whereas fewer vibrational states are available to a rigid conformation.

The energy landscape theory of protein folding is a statistical description of the protein potential surface (Onuchic et al., 1997). Although the overall energy landscape of a foldable protein can be described by a few parameters characterizing its statistical topography, in reality the number of degrees of freedom of a polypeptide is huge, $3N - 6$, where N is the total number of atoms. Not all degrees of freedom contribute to the folding reaction coordinates, which are mainly torsional motions of the polypeptide backbone. Nevertheless, characterizing the energy landscape is still an extremely difficult task.

Fig. 1 *a* illustrates the concepts of sharp and flat potential energy surfaces and their corresponding vibrational levels. In a rigid potential well, a molecule has a high vibrational frequency at room temperature, with a concomitant lower vibrational entropy. In contrast, a flat potential energy surface allows more vibrational states at room temperature, corresponding to higher vibrational entropy. Thus, the vibrational entropy of a given protein in a particular conformation indicates the shape of the potential energy surface near the respective local minimum. A change in the vibrational entropy of the folding polypeptide chain reflects a change in the shape of the folding energy landscape. Note that Fig. 1 *a* corresponds to the Levinthal concept of protein folding, in which the folded state is unique and rigid, whereas the denatured states are in the shallow flat potential wells. The new concept of folding funnel-like energy landscape, as in Fig. 1 *b*, predicts different vibrational features in protein folding.

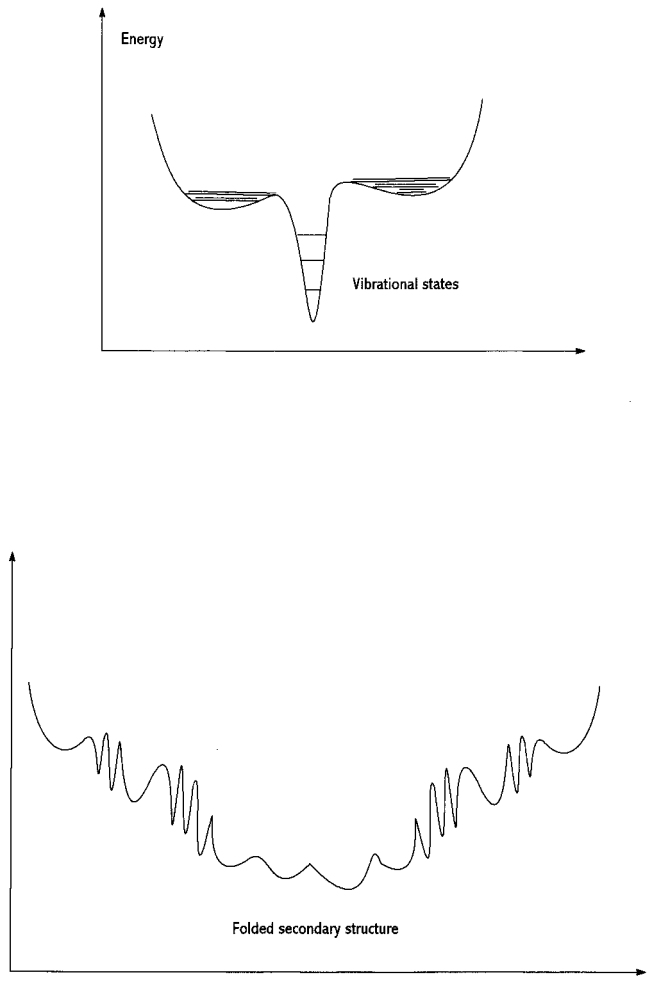

FIGURE 1 An illustration of the vibrational level and the energy landscape. (*a*) The traditional Levinthal landscape. (*b*) The landscape for secondary structure formation. This drawing reflects the finding that both α-helices and β-hairpins generally have softer vibrational motions than their corresponding random structures.

In this study, we examine the vibrational properties of protein folding in a systematic way. We start from protein secondary structure formation by studying short peptides. We proceed to study larger building blocks in protein folding and, finally, we examine large protein domains and small proteins.

THEORY AND METHODS

A rigorous description of protein folding must consider the solvation effect. However, the presence of solvating water molecules in the vibrational frequency calculation will produce considerable noise, with motions that are not related to the protein vibration. Hence, in our calculations, we consider only the vibrational contributions from the peptide chains, using a dielectric constant of D = 15*r to approximate solvent screening. The hydrophobic effect is ignored in the calculations.

All computations are performed using the Discover Molecular Modeling System, version 2.98 (BIOSYS/MSI, San Diego, CA) with the CFF91 all atom force field (Maple et al., 1998). All van der Waals interactions and electrostatic interactions are included in the energy minimization and second order derivations calculations, i.e., no distance cutoff is applied.

Native polypeptide conformations are taken from the PDB database without crystal waters. Hydrogen atoms, if missing in the deposited structure, are added using the biopolymer module in INSIGHTII package (BIOSYS/MSI, San Diego, CA). Random structures are generated by high temperature molecular dynamic simulations at 1000 K.

Before calculating the vibrational frequencies, each conformation is minimized with the conjugate gradient method with up to 30,000 iterations or to a gradient less than 10^{-4} kcal/mol*Å. With this level of minimization, it is sufficient to produce six zero-frequency modes (Max 0.02 cm^{-1}) and no negative eigenvalues are observed, i.e., each conformation is at a local minimum. The vibrational normal mode analysis has been carried out by solving the second-order derivations of the potential energy surface. All vibrational modes are included in our calculations, with harmonic approximations.

The vibrational contribution of the enthalpic and entropic components of the free energy are obtained in the standard way:

$$H_{\text{vib}} = \sum_{i=1}^{3N-6} \left[\frac{1}{2} + \frac{1}{e^{h\nu_i/KT} - 1}\right] h\nu_i$$

$$S_{\text{vib}} = \sum_{i=1}^{3N-6} \left\{\left[\frac{h\nu_i/KT}{e^{h\nu_i/KT} - 1} - \ln\left[1 - e^{-h\nu_i/KT}\right]\right]\right\}$$

where N is the total number of atoms in the peptide, ν_i is the vibrational frequency, h is Planck's constant, K is the Boltzmann constant, and T is the temperature.

The vibrational free energy for a given conformation is:

$$G_{\text{vib}} = H_{\text{vib}} - TS_{\text{vib}}$$

All calculations are carried out at room temperature (298 K). We partition the vibrational free energies into three contributions. First, we examine the vibrational free energies contributed from all $(3N - 6)$ vibrational modes. The vibrational frequencies of proteins/peptides range from low frequencies (a few cm^{-1}) to very high frequencies (3800 cm^{-1} for bond stretching involving hydrogen atoms). The vibrational free energies mainly derive from entropic contributions of low vibrational frequencies, i.e., less than 100 cm^{-1}. However, these low frequency vibrational modes are very sensitive to solvation effects. In solution, except for fibrous proteins, the low frequency vibrations may be easily lost and transformed into fluctuating stochastic motions. Second, therefore, we are also interested in the vibrational free energies contributed from modes higher than 20 cm^{-1} and, third, those contributed from modes higher than 50 cm^{-1}. Vibrational free energies not including motions below 20 cm^{-1} may represent the vibrational properties of polypeptides in a more consistent manner. It should be noted that these lowest modes are important and may couple to large scale conformational transitions. A better approach toward removing the noise introduced by the presence of solvent molecules might be through calculations of effective normal modes from solvated molecular dynamics simulations.

Kitao et al. (1998) have shown that the energy surfaces of individual protein conformational substates are nearly harmonic. Furthermore, we expect that small anharmonic corrections present in both the native and the random states will cancel out (Tidor and Karplus, 1994). In this study we focus mainly on the vibrational correction of the folding energy and the steepness and flatness of the energy landscape. Accurate description of the energy landscape needs to consider the solvation effects. Thus, we only report the vibrational free energy rather than compare the relative free energies of random and native conformers.

RESULTS AND DISCUSSION

Change of vibrational frequency in protein folding

One interesting vibrational feature of peptides/proteins is the amide I′ mode and the N-H stretch mode. The amide I′ mode arises predominantly from the vibration of the carbonyl C=O stretch. This bond is sensitive to environmental change and is often used to monitor secondary structure formation. A rigorous assignment of the protein amide I′ bands from equilibrium infrared (IR) spectra to specific secondary structure elements is currently an active area of research (Williams et al., 1996). N-H stretch modes were also used to monitor β-hairpin formation (Haque et al., 1996). In the present work, the CFF91 force field reproduces the amide I′ band in the 1600–1700 cm^{-1} region, and the N-H stretch around 3400 cm^{-1}. Experimental IR shift is also approximately reproduced. In this regard, we focus on a small 21-residue α-helical peptide, $AAAAA(AAAARA)_3A$. Experimentally, a similar peptide, the so-called suc-F_s 21-peptide: Suc-$AAAAA(AAAARA)_3A$-NH2, was well characterized (Williams et al., 1996). The IR spectra for the unfolding of the suc-F_s 21-peptide shows a sharp decrease of the peak at 1633 cm^{-1} and a slight increase of the peak at 1672 cm^{-1} (Williams et al., 1996). Consistently, our computed IR spectra show that the peak around 1606 cm^{-1} decreases sharply and the peak around 1697 cm^{-1} increases slightly upon the unfolding of the peptide $AAAAA(AAAARA)_3A$ (Fig. 2). The ± 20 cm^{-1} deviations between computed and experimental peak position are expected within the force field accuracy. Note that our calculations use only a distance-dependent dielectric constant to approximate the solvation effect. It is encouraging that our study reproduces the pattern of the experimental IR spectra for the folding-unfolding of the suc-F_s 21-peptide. Therefore, even though the present force field and the computational methods available are insufficient for an accurate comparison of the computations with spectroscopic data for proteins (Elber, 1996), the force field we used still captures the essential features of the vibrational change during the peptide folding process.

Fig. 3 *a* illustrates the vibrational frequency shift for the folding of the leucine zipper (c-Myc-Max heterodimeric leucine zipper, 2a93; Lavigne et al., 1998). We have calculated the vibrational frequencies for the average NMR structure and for six individual NMR structures. The native states

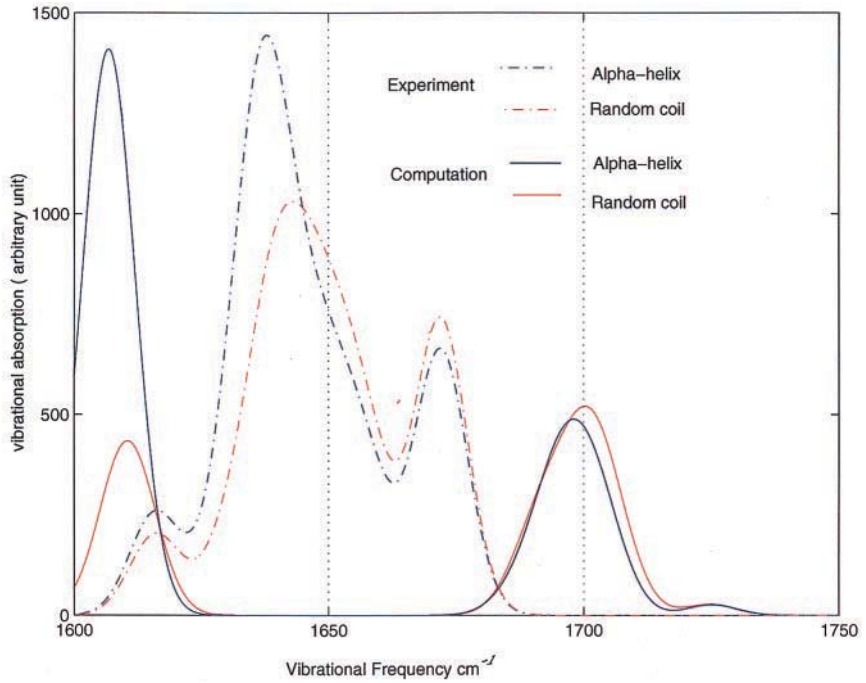

FIGURE 2 Comparison of the theoretical and experimental IR spectra of the suc-Fs 21-peptide. The theoretical spectra is constructed from a function of $[I_{vib} = \Sigma_{X=1}^{1800} \Sigma_{i=1}^{3N-6} [I_i e^{-0.02*(\nu_i - X)^2}]]$ where I_{vib} is the vibrational intensity of frequency X, X is a grid with a 0.1 spacing between 1 and 1800 cm^{-1}, ν_i is the normal mode vibrational frequency obtained from the second derivative calculation, and I_i is its vibrational intensity.

have similar vibrational spectra, with a small degree of variation. The random structures are generated by high temperature molecular dynamics simulations. Fig. 3, *a* and *b*, shows that the different random structures have very similar folding patterns. On the other hand, the dimerization of the leucine zipper monomer (blue line) illustrates a different shift. As is evident from Fig. 3, the vibrational frequencies do not shift uniformly downward or upward in the folding process. Depending on the vibrational motion, it could be either an upshift or a downshift.

The vibrational frequency shift in protein folding is sensitive to both the three-dimensional folding pattern and to the protein sequence. Fig. 4 *a* shows that, as expected, different proteins have different folding frequency shifts. Fig. 4 *b* indicates that the same folding domain (the SH3 domain in our case here) may also have different folding frequency shifts, depending on the sequences of this protein. However, the variation in the vibrational shift for the same domain with different sequences is smaller than that of different 3-D folds.

In general, there are two sources for vibrational frequency shifts in protein folding, i.e., local and global. Local factors include torsional changes in the backbone conformation, breakage or formation of hydrogen bonding, and local electrostatic effects. Local effects involve strong interactions and reflect shifts in both high and low frequency regions.

The global factors may include long range electrostatic interactions and cooperative interactions between different regions. These effects are likely to be involved mainly in low frequency motions. As for a measure of the rigidity or flatness of the folding energy landscape, vibrational shifts in a low frequency region (0–200 cm^{-1}) might be the more relevant ones. As shown in Fig. 3, vibrational frequency shifts for the folding of different random structures of the leucine zipper differ mainly in the region of less than 100 cm^{-1}. Vibrational motions of less than 100 cm^{-1} contribute substantially to vibrational thermodynamic changes in protein folding.

Secondary structures of peptides

To investigate the vibrational properties of short peptides, we compute the vibrational frequencies of 40 peptides (with fewer than 30 residues for each peptide) in both the folded and the random states. Available x-ray crystal and NMR structures of the peptides are extracted from the PDB database. For the crystal structures, we compute the vibrational frequencies for the native structure. For the NMR structures, we calculate the vibrational frequencies for several folded conformers and average their vibrational free energies. The random structures are generated by high temperature molecular dynamics simulations at 1000 K. Five random structures are generated for each peptide, and their vibrational spectra are subsequently calculated. The larger the number of random structures, the more representative would be the description of the unfolded structure. However, we found that using five random structures already gives a good representation and is computationally efficient. The vibrational free energies of the five random structures are averaged and taken as a measure of the energy landscape of the random states. This allows us to compare the relative vi-

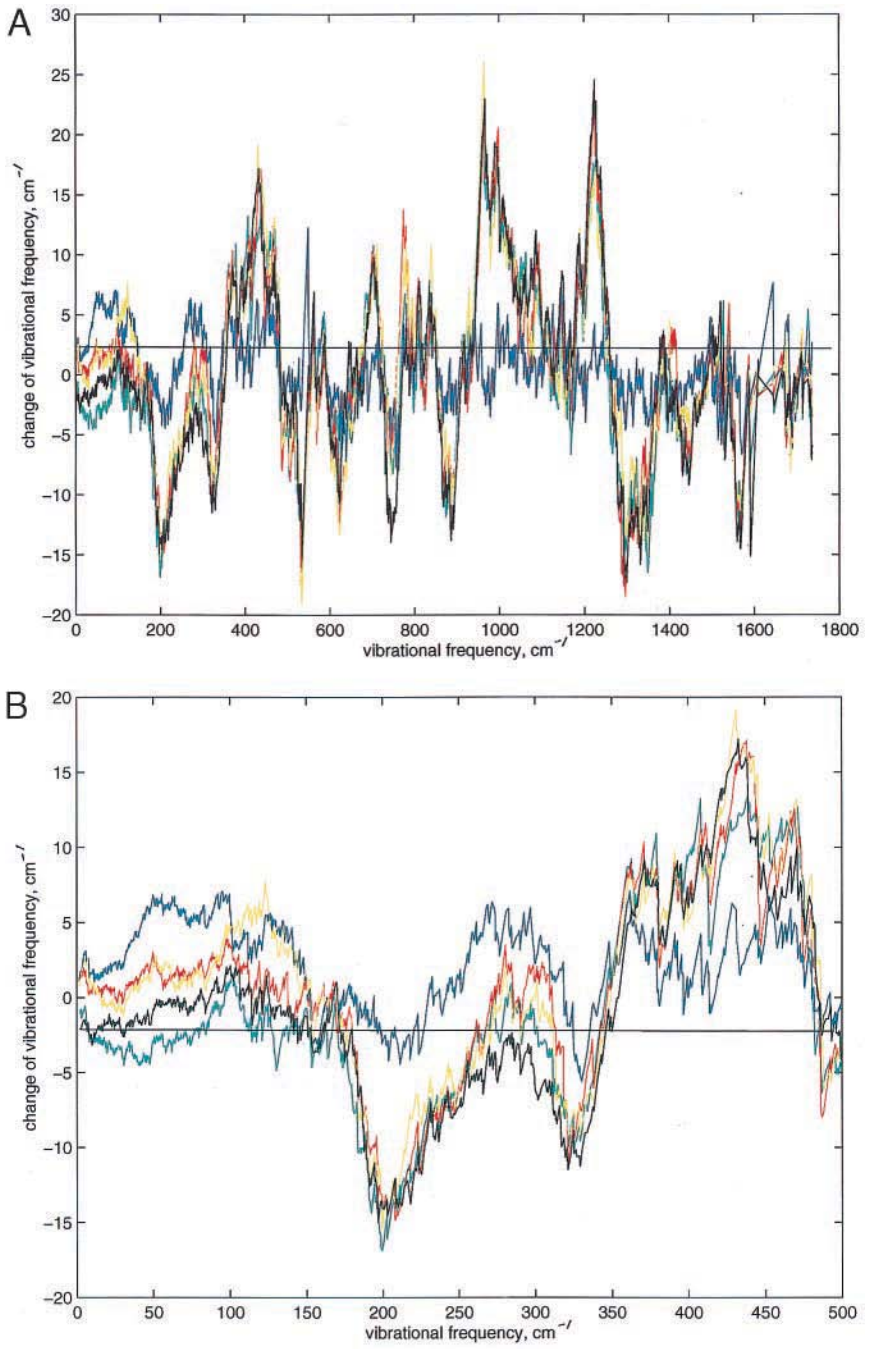

FIGURE 3 The change in the vibrational frequencies upon folding of the c-Myc-Max heterodimeric leucine zipper. Blue line indicates the dimerization of monomeric conformer, and other colors refer to the folding of four of the random structures. (*a*) Whole spectra (with high frequencies involving hydrogen atoms omitted). (*b*) Enlargement of the low frequency region.

brational free energies of the native and random states. If the random structures have higher average vibrational free energies than the native states, the folded states are likely to be more flexible than the random structures. And, conversely, if the native structures have higher average vibrational free energies than the random structures, then the native folded states are more rigid than the random states.

Table 1 reports three types of vibrational free energies for seven α-helices, eleven β-hairpins, and ten loop structures (Ishikawa et al., 1999). Interestingly, we observe that most of the folded secondary structures have lower vibrational free energies than random structures. Hence, both α-helices and β-hairpins are vibrationally more flexible than random structures. The traditional view of the vibrational properties of peptide secondary structures concerns mainly α-helices. Compared with random structures, α-helices can gain low vibrational frequencies for longitudinal modes, explaining the low frequency motions of α-helices. For β-hairpin structures, it appears that the opening and closing of the β-strands also correspond to low frequency vibrational mo-

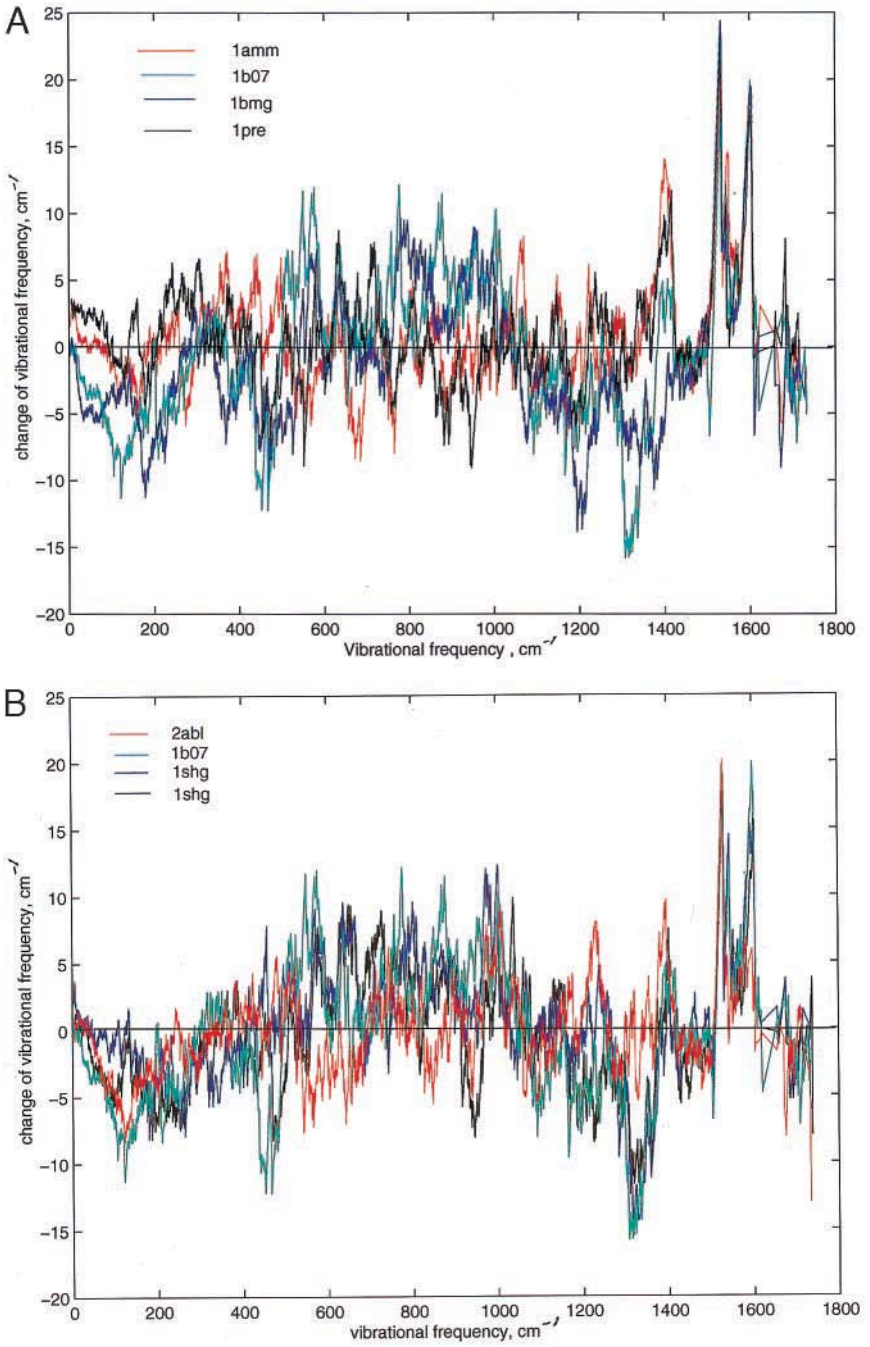

FIGURE 4 (*a*) The change in the vibrational frequencies upon folding of several proteins. One random conformer is chosen as the unfolded structure for each protein. (*b*) The change in the vibrational frequencies upon folding of the SH3 domain with different sequences. One random conformer is chosen as the unfolded structure for each of the proteins, 2abl (red) and 1b07 (green). For 1shg, two random structures are used (blue and black).

tions. There is, however, a significant difference between the vibrational spectrum of α-helices and that of β-hairpin structures. For an α-helix, the contribution of ΔG_{vib} comes exclusively from motions less than 20 cm^{-1}, the contributions from the modes higher than 50^{-1} average to be -0.1 kcal/mol. However, for β-hairpin structures, one-third of the ΔG_{vib} comes from vibrations higher than 50 cm^{-1} (Table 1, average vibrational free energy corrections for all modes is 4.2 kcal/mol, and 1.5 kcal/mol for the modes higher than 50 cm^{-1}).

If both α-helices and β-hairpin structures have favorable vibrational free energies, what is the situation for loop structures? Looped peptides usually do not have well defined structures in solution. However, some small peptides with disulfide bonds have NMR structures. We have studied nine such small peptides, and the results are reported in Table 1. "Native" loop structures do not have favorable vibrational free energies. Among the peptides, only 1scy (neurotoxin scyllatoxin, Martins et al., 1990) has a well defined secondary structure (Fig. 5). As Table 1 shows, 1scy

TABLE 1 Average vibrational free energy corrections (Kcal/mol) for short peptides

Pdb/sequence*	Number of residues	Secondary	RMSD† (Å)	All modes‡	20 cm^{-1} cut‡	50 cm^{-1} cut‡
1ale	18	α-helix	7.5	12.4	−3.9	−0.7
1dep	15	α-helix	4.5	5.0	1.4	−1.2
1odr	20	α-helix	6.8	6.1	2.9	−0.5
1btr	21	α-helix	7.9	3.7	0.1	1.6
1sol	20	α-helix	5.9	6.1	−0.9	−1.0
1fac	21	α-helix	6.0	3.6	2.7	0.5
1pei	22	α-helix	6.5	8.2	1.7	0.9
Average				**6.4**	**0.6**	**−0.1**
1azu (gln107-lys128)	22	β-hairpin	6.7	5.3	2.0	0.7
1cac (leu57-phe70)	14	β-hairpin	5.0	0.8	2.7	2.8
1cac (asp75-gln92)	18	β-hairpin	5.7	5.5	1.6	1.5
1cac (trp192-val211)	20	β-hairpin	6.8	7.3	4.7	3.0
2act (gly168-val180)	13	β-hairpin	4.8	3.7	−1.7	1.4
2alp (phn45-gly59)	18	β-hairpin	7.2	7.0	2.4	1.2
2alp (thr87-ser107)	16	β-hairpin	6.2	3.8	−1.3	1.9
2alp (leu119-ser124)	16	β-hairpin	6.0	10.2	1.5	1.8
2alp (arg138-gln158)	9	β-hairpin	4.3	−2.3	1.6	0.8
2apl (val167-gly170)	12	β-hairpin	5.3	1.5	2.8	0.8
2lyz (gln41-trp62)	22	β-hairpin	7.2	3.0	0.5	0.0
Average				**4.2**	**1.5**	**1.5**
1wbr	17	loop	5.3	−1.1	3.0	1.4
1pao	18	S-loop	5.2	3.2	0.3	1.5
1edp	17	S-loop	4.5	1.5	−1.4	−1.3
1fge	20	S-loop	5.9	−1.9	−3.7	0.2
1ter	21	S-loop	5.0	1.8	0.8	1.0
1omg	25	S-loop	4.7	1.0	0.3	2.4
1ans	27	S-loop	5.6	−2.3	1.0	0.5
2eti	28	S-loop	6.0	0.8	5.8	1.5
1mmc	30	S-loop	6.6	0.8	0.9	0.4
1scy	31	α + β	6.9	4.0	1.0	1.0
Average				**0.8**	**0.8**	**0.9**

Vibrational free energy correction: $\Delta G_{vib} = G_{vib}$ (random) $- G_{vib}$ (native). Positive ΔG_{vib} indicates a flexible native state.
*Pdb code and real sequences were used in calculations.
†RMSDs are the average of RMSDs between the random conformers from the simulations versus the native conformer.
‡All modes: all vibrational ($3N - 6$) modes are used in calculation of vibrational free energy. 20 cm^{-1} cut: Only the frequencies higher than 20 cm^{-1} are included in the calculation. 50 cm^{-1} cut: Only the frequencies higher than 50 cm^{-1} are included in the calculation. These notations are the same for rest of tables.

is one of the two peptides with favorable vibrational free energies.

Building blocks and domains

Folding is a hierarchical process (Baldwin and Rose, 1999a,b), involving a combinatorial assembly of a set of conformationally fluctuating building blocks (Tsai et al., 1999a). A building block is a fragment of the protein, with a transient, highly populated conformation. Building blocks associate into hydrophobic folding units, which further associate to form domains and, subsequently, entire proteins (Tsai and Nussinov, 1997). The initial formation of "microdomains" in protein folding in the collision-diffusion model is also characterized by features similar to the formation of building blocks. The foldon approach (Panchenko et al., 1996), where a protein is built from an assembly of foldons, also corresponds nicely to the building blocks concept.

Starting from the native structure, a protein is progressively cut into smaller units, culminating in a set of building blocks. The sizes of the building blocks range from 15 to >100 residues. The smaller usually involve a few secondary structure elements, and the larger usually form a separate domain. According to the compactness, hydrophobicity, and isolatedness (Tsai and Nussinov, 1997), a score is computed for each building block to indicate its stability. The higher the cutting score, the more stable the building block is supposed to be. Based on the cutting score, we picked 14 building blocks with the scores ranging from 1.4 to 8.2 (Table 2, Fig. 6) and computed their vibrational properties. Random structures are again generated by high temperature molecular dynamics simulations. We divide the denatured simulated structures into two groups, one with low RMSDs

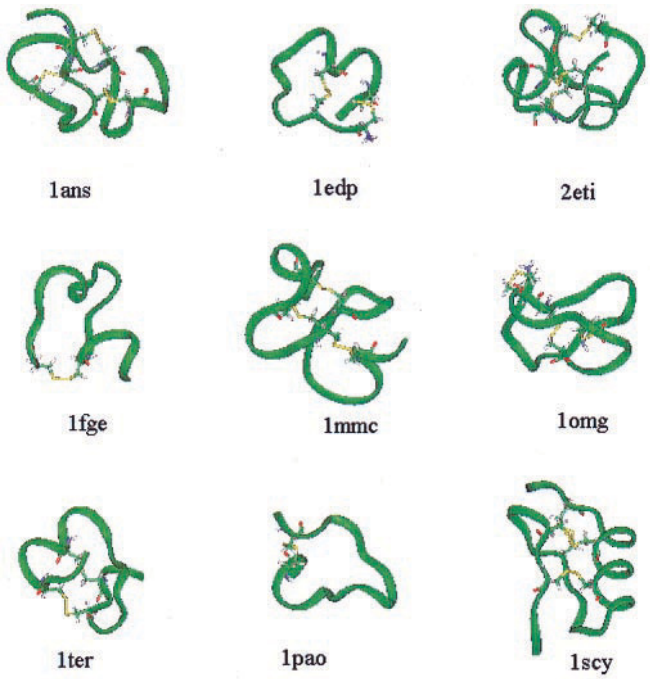

FIGURE 5 An illustration of the conformations of folded peptides with disulfide bonds.

as compared to the native structures and the other with high RMSDs. The low RMSD structures are close to the native on the energy landscape, whereas the high RMSD structures represent structures further away from the native states.

Table 2 lists six building blocks with cutting scores under 5.0 (Fig. 6 *a*). Five of these small building blocks (except 1shc, Martins et al., 1990) are combinations of short α-helices. A comparison of the vibrational properties of these five building blocks with straight α-helices (Table 1) indicates a profound change in their energy landscape. The average vibrational free energy difference between the random and the native state for straight α-helices is 6.4 kcal/mol (Table 1). It decreases to -0.9 for this group of peptides. However, the contributions from the higher frequency motions (larger than 20 cm^{-1}) is still the same (0.6 kcal/mol for α-helices in Table 1, 0.5 kcal/mol for the distorted α-helix blocks in Table 2).

Moving down to the second half of Table 2, there are 8 building blocks/domains with cutting scores above 5.0 (Table 2, Fig. 6 *b*). The vibrational properties of these 8 differ both from those of the small building blocks and from those of the simple secondary structures. Table 2 shows that on average, for all vibrational motions, large building blocks/domains have more rigid native structures compared with random structures. However, if we discard the low frequency motions (those under 20 cm^{-1}), native structures have lower vibrational free energies than random structures. Hence, this suggests that with respect to the large scale low frequency motions, the native structures are less flexible than the random structure. However, with respect to the higher frequency smaller scale motions, the native structures are more flexible.

Is there a correlation between the cutting scores of the building blocks and the vibrational free energies? The higher the cutting score, the more compact and the more stable the building block. Consistently, we observe a correlation between the cutting scores and the vibrational free energies. However, this correlation may be due to a correlation between the sizes of the peptides and the vibrational frequencies.

Conventional wisdom suggests that the unfavorable vibrational free energy contribution to protein folding increases with the size of the peptide/protein. Fig. 7 illustrates that this is the case here, too. Khechinashvilli et al. (1995) have used an empirical partition method to fit the experimental heat capacity change for protein unfolding. The trend they obtained is similar to that shown in Fig. 7.

It is interesting to compare Fig. 7 *a* with Fig. 7 *b*. If we do not include the contributions from the low vibrational motions (<20 cm^{-1}), we notice that the trend in the change in the vibrational free energies is opposite to that observed when we include all vibrational motions. This indicates that motions under 20 cm^{-1} still contribute significantly to the thermodynamics of protein folding in solution, even though these low frequency motions are vulnerable to the solvation effects. This is also an indication of the sensitivity of the energy landscape to a change in the environment (Kumar et al., 2000a). Changes in the viscosity and other solvent dynamic properties can affect the low frequency vibrations and thus affect the energy landscape.

Folding energy landscape: from small segments to large domain and protein

The formation of a building block can be described by a microfunnel-like energy landscape. At the bottom of the microfunnel there is an ensemble of conformations of building blocks. Via combinatorial assembly, building blocks bind to form a stable, higher-population time conformation, i.e., the hydrophobic folding unit. In terms of the folding funnel landscape, the entire folding/binding process may be viewed as sequentially fusing and modifying individual funnels (Tsai et al., 1999a). Therefore, a study of the shape of the microfunnel-like energy landscape of the building block is informative with respect to the energy landscape during the folding process.

Starting from a random structure, the formation of a secondary structure (an α-helix or a β-sheet/hairpin) is an important step in protein folding. The microfunnel-like energy landscape for this step (Fig. 1 *b*) is characterized by a flat bottom. This type of microfunnel is deduced from the overwhelmingly favorable vibrational entropy for both α-helices and β-sheet/hairpin structures, and is consistent

TABLE 2 Vibrational free energy (kcal/mol) for building blocks/domains

Pdb/sequence*	Number of residues	Cutting scores	RMSD (Å)†	All modes	20 cm^{-1} cut	50 cm^{-1} cut
1shc (A: gly13-gly37)	26	1.4	4.8	−5.1	−0.8	2.1
			6.9	−8.1	−1.8	2.1
1sra (met150-lys187)	38	2.3	5.8	11.5	0.5	0.6
			9.5	8.7	−1.5	−3.0
1bmt (A: glu653-ala682)	31	2.4	4.9	−2.1	3.1	1.0
			6.3	−2.3	3.1	1.0
1occ (F: pro7-pro30)	24	2.4	4.5	−7.4	1.2	0.2
			7.2	−0.4	−0.2	−1.3
1aab (met12-ser52)	41	3.3	6.5	6.1	−1.4	0.0
			9.4	−4.7	1.5	1.6
1qrd (A: ser51-ser81)	31	3.5	4.8	−2.2	1.4	2.6
			8.2	−4.5	1.3	1.4
Average				**−0.9**	**0.5**	**0.7**
1ryt (val147-ile189)	43	5.7	4.0	7.1	0.2	−0.9
			10.5	−3.8	3.5	0.4
1div (met1-gln55)	55	5.9	6.2	−7.7	0.9	2.8
			11.0	−2.1	0.4	−3.6
1efu (A: lys9-gly41)	33	6.2	7.6	−2.3	3.9	1.0
			8.8	−2.9	3.9	2.5
1uxd (met1-his48)	48	6.2	6.0	0.4	3.7	−0.7
			10.0	−4.2	1.8	−1.5
2abl (SH3 domain)	68	6.3	5.5	0.2	4.5	5.5
			12.4	−4.8	4.8	5.6
1pre (B2: glu2-asn79)	78	8.0	4.7	−9.0	3.0	5.4
			12.6	−14.9	2.7	3.7
1amm (gly1-leu80)	80	8.0	5.1	−4.8	11.1	2.5
			13.4	−8.2	8.0	−1.1
1lmk (val2-ser127)	126	8.2	6.5	2.6	16.3	2.7
			16.7	−5.0	18.8	1.3
Average				**−3.7**	**5.5**	**1.6**

Vibrational free energy correction: $\Delta G_{vib} = G_{vib}$ (random) $- G_{vib}$ (native). Positive ΔG_{vib} indicates a flexible native state. The first small building blocks have small cutting scores and are supposed to be less stable. The second set is about larger building blocks with large cutting scores and are supposed to stable.

*Pdb code, the chain, and the real sequences used in calculations. 1shc (A: gly13-gly37) refers to pdb code 1 shc, chain A from gly13 to gly37.

†RMSDs are the average of RMSDs between the random conformers from the simulations versus the native conformer.

with the flexible nature of the secondary structures. In the next step of the folding events, secondary structures may combine, merging the microfunnels to form small building blocks. Here we observe a variable behavior: whereas α-helices appear to strongly rigidify the resulting building block (Fig. 6 *a*, Table 2), β-hairpin assembly to form a β-sheet still allows soft vibrational motions. The formation of large building blocks, or of isolated protein domains, generally locks and rigidifies small building blocks. The present study provides such examples, e.g., protein G (1gb1), ubiquitin (1ubq), and the prion protein (1ag2; Fig. 9). Table 3 illustrates that these proteins have higher vibrational energies than the average random structures. However, certain types of protein structures still allow a flexible funnel bottom, for example, β_2-microglobulin (1bmg) and the SH3 domain (1b07). Hence, although the vibrational properties of protein/peptide folding may progressively rigidify the energy landscape, they may also enable flexibility.

The formation of the leucine zipper dimer is a good example to illustrate the formation and assembly of α-helices. Fig. 8 shows ten leucine zipper conformers and their relative vibrational free energies. The leucine zipper dimer is formed by connecting monomeric leucine zippers by a disulfide bond. Therefore, there is no rotational and translational change in the dimerization. The linear leucine zipper monomer has the lowest vibrational free energy. Highly coiled random structures are about 35 kcal/mol higher in vibrational energy. Therefore, the formation of the leucine zipper monomer corresponds to a change from a narrow energy microfunnel (the coiled random structures) to a broad flat bottom (the monomeric leucine zippers). The formation of the dimer strongly rigidifies the funnel, since the coiled coil dimer has a much higher vibrational free energy. The rigidification has two reasons: First, several salt-bridges are formed between the two α-helices (Lavigne et al., 1998). And second, the binding of two α-helices makes it difficult for the two α-helices to vibrate in phase, and hence, they lose their low vibrational frequencies for longitudinal modes. Similar types of merging of microfunnels are observed for the small building blocks in Fig. 6 *a*.

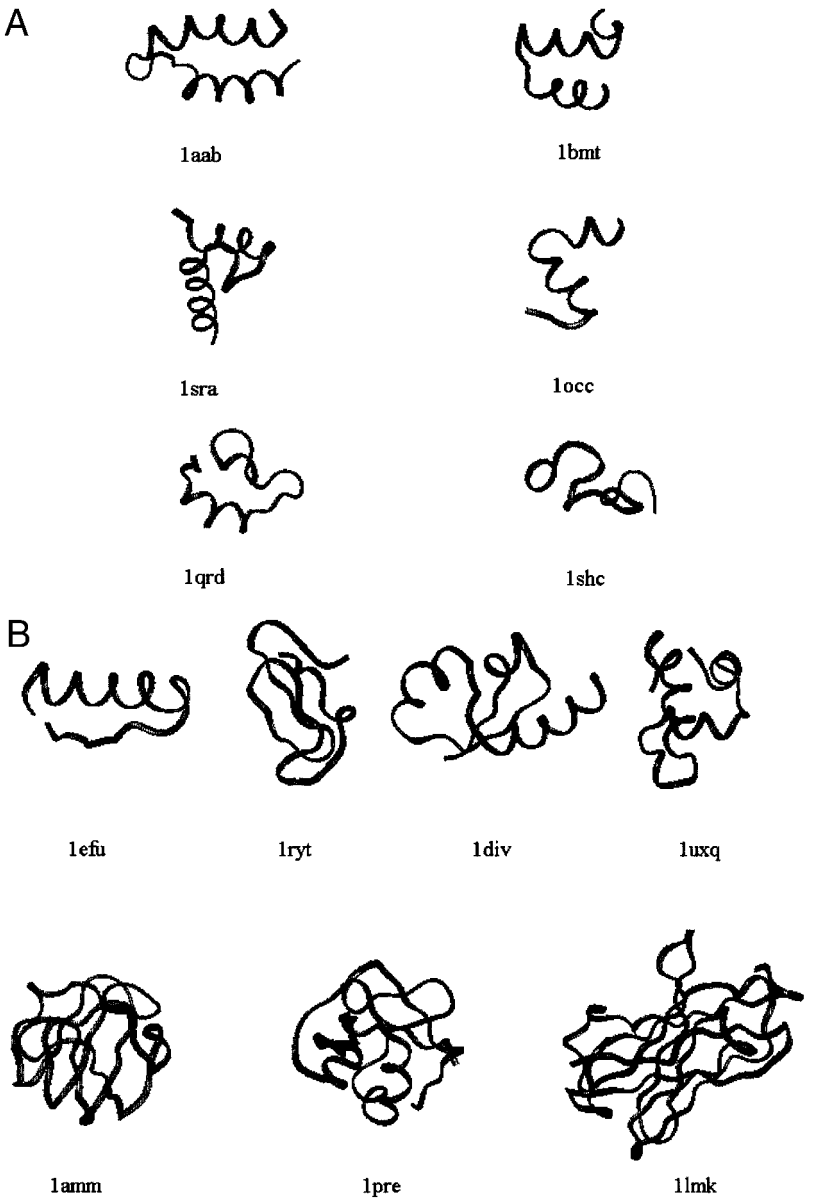

FIGURE 6 Backbone conformations of building blocks. (*a*) Building blocks with low scores. (*b*) Building blocks with high scores.

The formation and assembly of β-sheet/hairpin structures has been investigated by cutting SH3 domains. The SH3 domain consists mainly of β-structures (for example, PDB code 1b07 in Fig. 9). Viguera et al. (1996) studied the solution conformations of peptides that span the entire length of the α-spectrin SH3 domain. There are three separate β-hairpins (peptides m4, m6, and m8, Table 4), and peptide m68, which is the composite of m6 and m8. The CD and NMR results indicate that none of the peptides populate, to a large extent, a particular secondary structure conformation. However, a careful analysis of the NMR data reveals that peptides m6, m8, and m68 could adopt native-like conformations to some extent. Therefore, these peptides could be small building blocks in the folding of the SH3 domain. In our vibrational analysis of peptides m4, m6, m8, m68, and the SH3 domain itself (1shg), we see that the microfunnels of m4, m6, and m8 should have flat bottoms, since all have small vibrational free energies. Merging the microfunnels of two β-hairpins (m6 and m8) produces a similar flat microfunnel of peptide m68. Finally, merging all microfunnels yields the funnel of the SH3 domain, which also has a relatively soft (flexible) funnel bottom. We have studied three sequences of SH3 domains (1shg, 1b07, and 2abl, Fig. 4 *b*). Of the three, the funnel of 1b07 is the softest (Table 3) and that of 2abl (Table 2) is semi-rigid.

Hence, unlike in the case of the leucine zipper dimer, whose funnel rigidifies after the binding and fusing of the two flatter microfunnels of the α-helical monomers, the β-sheet domains appear likely to have soft funnel bottoms. In addition to the SH3 domains discussed above, the β-sheet

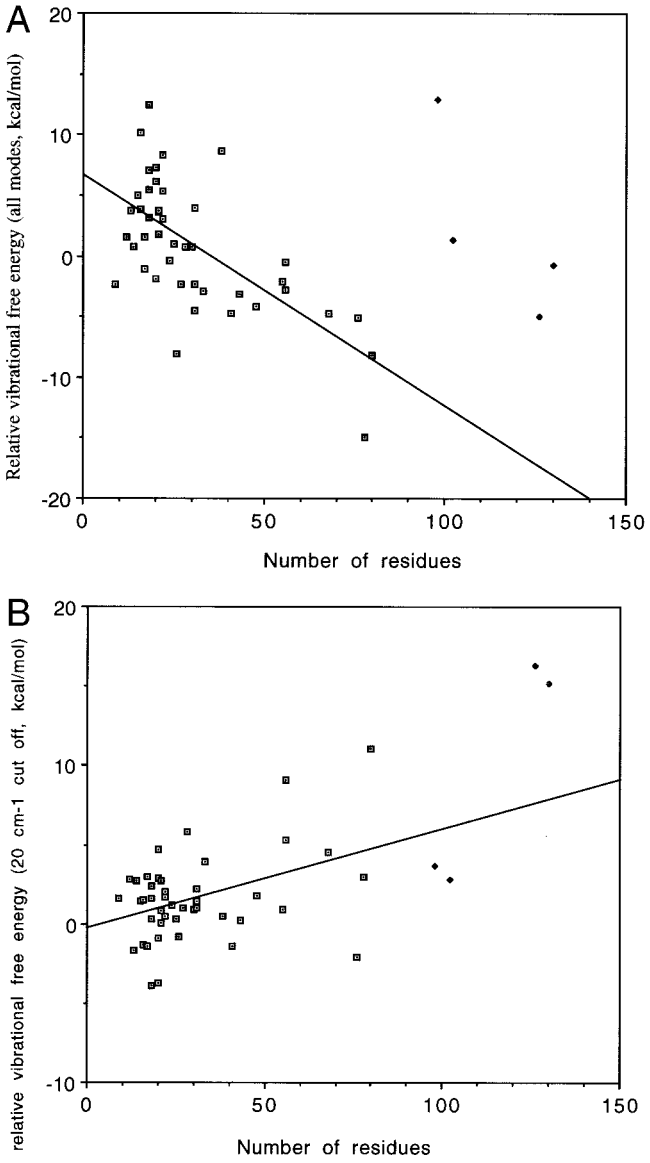

FIGURE 7 Correlation of the vibrational folding energy with protein size. Large proteins are omitted due to insufficient data (indicated by blue diamonds). (*a*) The vibrational folding energy includes all vibrational modes. (*b*) The vibrational folding energy includes vibrational modes higher than 20 cm^{-1}.

domain of β_2-microglobulin (1bmg, Table 3) clearly suggests that it is a domain with a potentially flexible funnel bottom. We have simulated the unfolding trajectory of 1bmg by molecular dynamics simulations. The unfolding of 1bmg shows a nice picture of the opening and flipping of the building blocks (Kumar et al., 2000a; B. Ma and R. Nussinov, unpublished manuscript). Thus, an examination of the vibrational free energy change along the unfolding trajectory of this β_2-microglobulin (1bmg) might provide information on its folding funnel. We calculated the vibrational properties of 19 conformers along the unfolding trajectory of the β_2-microglobulin (1bmg, with RMSDs ranging between 4.0 and 13.5 Å, B. Ma and R. Nussinov, unpublished manuscript) and 9 randomly generated conformers (RMSDs ranging from 13.0 to 16.8). The change of the vibrational free energy with RMSDs from the native conformations are plotted in Fig. 10. As seen in Fig. 10, conformers that are far from the funnel bottom (larger RMSDs) have considerably larger vibrational free energies (more rigid) than the small RMSD conformers. The folding funnel of 1bmg corresponds to an energy landscape with a steep well and a flat bottom, illustrating its flexibility around the native state.

TABLE 3 Vibrational free energy for large domains

Pdb/sequence*	No. of residues	RMSD (Å)†	All modes	20 cm^{-1} cut	50 cm^{-1} cut
1gb1 (protein G)	56	9.8	−2.8	5.3	−0.7
1b07 (sh3 domain)	58	8.9	2.0	7.7	−2.6
		11.7	6.5	9.4	−1.7
1ubq (ubiquitin)	76	5.7	−5.6	−2.1	−0.7
		12.5	−5.1	−3.6	−4.5
1ag2 (prion)	102	10.4	−8.7	2.6	2.9
		14.0	1.3	−2.1	−0.5
1lz1 (lysozyme)	130	6.3	−0.7	15.2	10.1
1bmg (microglobulin)	98	7.7	3.7	3.7	1.6
		14.1	12.9	13.0	3.9

Vibrational free energy correction: $\Delta G_{vib} = G_{vib}$ (random) $- G_{vib}$ (native). Positive ΔG_{vib} indicates a flexible native state.
*Pdb code, the chain, and the real sequences used in calculations.
†RMSDs are the average of RMSDs between the random conformers from the simulations versus the native conformer.

Contribution of vibrational free energy to protein folding

Previously, in a study of the relative conformational free energies of a β-hairpin peptide, we (Ma and Nussinov, 1999) found that β-hairpin conformations for that particular peptide generally have large vibrational entropy that contributes substantially to the stability of folded β-hairpin structures. The present study extends these results and illustrates that both α-helices and β-hairpin secondary structures have large vibrational entropies. Favorable vibrational entropy may play a role in protein folding and unfolding. Folded protein/peptide structures usually lose enormous conformational entropy. However, it may be compensated by the gain of vibrational entropy. At room temperature, there may be a balance between the loss of conformational entropy and the gain of vibrational entropy. However, at high temperatures, the gain of vibrational entropy is outpaced by the loss of conformational entropy, and the protein is unfolded. At low temperatures, the favorable positive vibrational entropy might, however, lose its effect. This situation of low vibrational entropy at low temperatures might relate to the interesting phenomenon of cold denaturation.

The results obtained here suggest favorable vibrational free energy corrections (i.e., positive ΔG_{vib}) for both α-he-

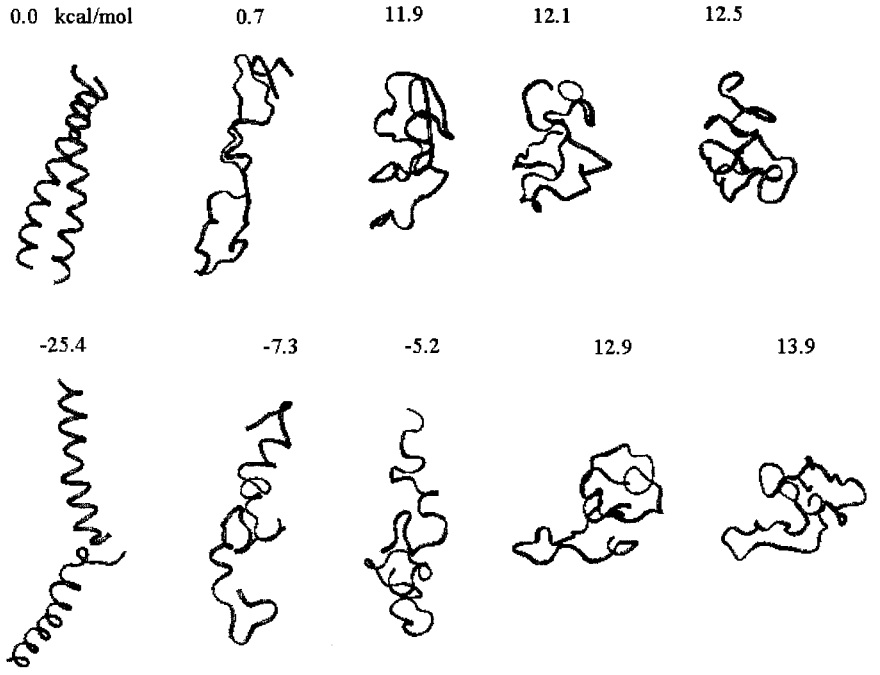

FIGURE 8 Backbone conformations and relative vibrational folding energy for ten conformers of the c-Myc-Max heterodimeric leucine zipper.

lices and β-hairpin secondary structures. Since, for a small peptide, the loss of conformational entropy is relatively small, this result may be more relevant for a small peptide. If we take the total configurational entropy lost upon folding to be about 41 J.K/mol per residue (Makhatadze and Privalov, 1996), this translates to about 60 Kcal/mol for a 20-residue peptide. Thus, the vibrational correction is about 10% of the conformational entropy which is lost. On the other hand, in large proteins, the contributions of vibrational free energies vary from case to case. In large proteins the loss of conformational entropy increases enormously, and make the vibrational contribution much less important. Overall, the vibrational free energy favors unfolded random structures for large proteins, as indicated in the present study and previous ones (Sturtevant, 1977; Kanehisa and Ikegami, 1977; Khechinashvilli et al., 1995). For example, ubiquitin has been shown to undergo both heat- and cold-induced denaturation (Wintrode et al., 1994; Ibarra-Molero et al., 1999). Consistently, in the present study, we find that folded ubiquitin (1ubq) has unfavorable vibrational free energy. Experimental evidence (Wintrode et al., 1994; Ibarra-Molero et al., 1999) indicates that there is an enthalpic contribution to the cold denaturation of ubiquitin. In general, it has been suggested that cold denaturation is due

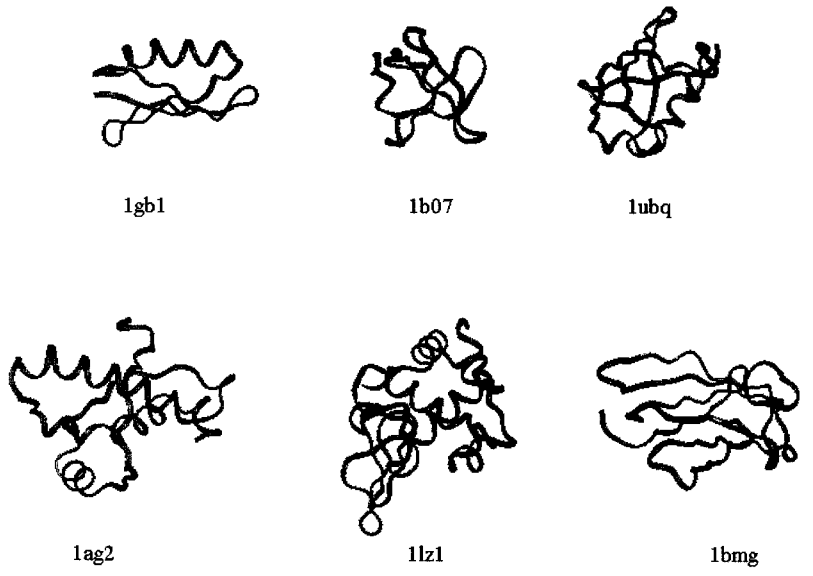

FIGURE 9 Backbone conformations of several proteins studied in this work.

TABLE 4 Vibrational free energy (kcal/mol) for SH3 domain and fragments

Pdb/sequence*	No. of residues	RMSD (Å)†	All modes	20 cm^{-1} cut	50 cm^{-1} cut
M4 (tyr13-asp29)	17	5.72	2.9	2.1	1.0
M6 (asp40-ala55)	16	6.4	3.2	3.2	−0.5
M8 (asp29-asp48)	20	5.8	5.1	1.6	0.1
M68 (asp29-ala55)	27	8.4	4.3	3.0	2.0
1shg (all)	56	6.1	−0.7	9.1	1.2
		12.3	−0.5	9.2	0.9

Vibrational free energy correction: $\Delta G_{vib} = G_{vib}$ (random) $- G_{vib}$ (native). Positive ΔG_{vib} indicates a flexible native state.
*Pdb code, the chain, and the real sequences used in calculations. 1shc (A: gly13-gly37) refers to pdb code 1shc, chain A from gly13 to gly37.
†RMSDs are the average of RMSDs between the random conformers from the simulations versus the native conformer.

to stronger energetic interaction of water molecules with amino acids previously buried in the protein interior (Graziano et al., 1997).

It is reasonable to assume that there is a hydrophobic contribution to cold denaturation. However, there is still a possibility of vibrational entropic origin. It is interesting to note that there are some peptides with folded secondary structures existing only at high temperatures which unfold at room temperature. Lacassie et al. (1996) synthesized a series of shorter peptides. At low temperature, these peptides and polypeptides are completely unordered. Upon heating, they undergo a reversible transition leading to a partly α-helical structure. In another example, Gursky and Aleshkov (2000) found that heating the soluble Alzheimer's β-amyloid peptide (Aβ) from 0 to 37°C induces a rapid reversible transition to a random coil + β-strand structure. Unfortunately, no thermodynamic analysis of these peptides has been reported.

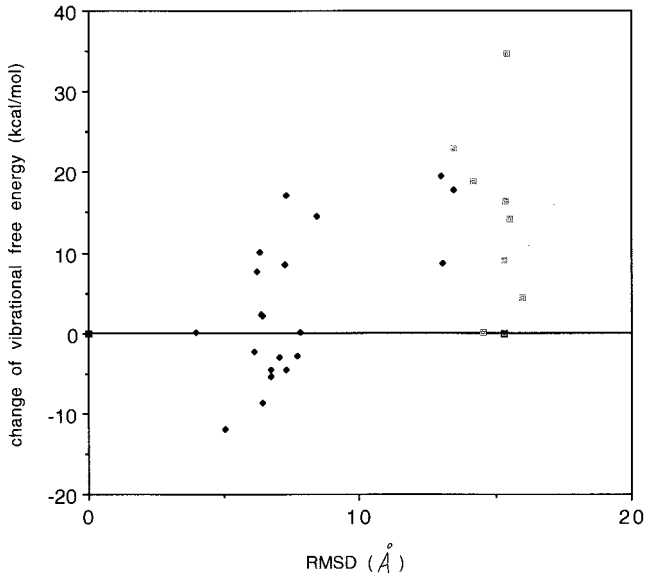

FIGURE 10 Vibrational folding energies for microglobulin (1bmg). The broad distribution of the random conformations are expected to represent the folding energy landscape. The positive numbers indicate rigid substates and negative data indicate flexible conformations. Blue dots represent the conformers along the unfolding trajectory, and the red dots are random conformers.

CONCLUSIONS

Molecular vibration, especially low frequency motions, may be used as an indication of the rigidity or the flatness of the protein folding energy landscape. Here we have studied the vibrational properties of native folded, as well as random coil structures of 40 peptides (with less than 30 residues for each peptide), 14 building blocks (ranging from 24 to 126 residues in length) and 7 small proteins (with sizes ranging from 56 to 130 residues). The picture we obtain from this systematic study of the vibrational properties of protein/peptide folding allows us to gain some understanding of how and why the energy landscape progressively rigidifies while still allowing potential flexibility.

Compared with random coil structures, both α-helices and β-hairpin structures are vibrationally more flexible. The vibrational properties of loop structures are similar to their corresponding random coiled structures. Furthermore, we find that the presence of an α-helix tends to rigidify peptides and building blocks, whereas inclusion of a β-structure has less effect. When small building blocks assemble into large domains, the protein rigidifies. However, some folded native conformations are still found to be vibrationally more flexible than random coiled structures (for example, β_2-microglobulin and the SH3 domain). Folding and binding are similar processes. Consistently, our computational results for protein folding are in agreement with the recent experimental finding that the backbone conformational entropy may also increase upon binding of a hydrophobic ligand (Zidek et al., 1999).

Our study indicates that hierarchical protein folding should be thermodynamically advantageous. The negative vibrational free energy change favors the formation of the local structures, such as α-helices and β-hairpins. The subsequent assembly of the building blocks into larger units rigidifies the protein structure. Thus, the process of coalescing of the preformed building blocks involves both a smaller vibrational entropy cost and a smaller conformational entropy cost than nonhierarchical processes. Recent studies of the transition-state ensemble indicate that the ensemble might be relatively homogeneous (Alm and Baker, 1999). This is consistent with the preformed building block conformations that assemble into the native structure, or into transient non-native contacts, in their trapped intermediate states.

Vibrational free energies contribute significantly to the thermodynamics of protein folding and to the distributions of the conformational substates. We find a weak correlation between vibrational folding energy with protein size, con-

sistent with previous experimental estimates and with theoretical partitioning of the heat capacity change during protein folding. For the leucine zipper dimer, the difference between the vibrational free energies of certain conformers can be as large as 35 kcal/mol, with the monomeric leucine zipper being vibrationally most flexible. Therefore, the formation of the leucine zipper monomer corresponds to a change from a narrow energy microfunnel (coiled random structures) to a broad flat bottom (monomeric leucine zippers). The formation of the dimer strongly rigidifies the funnel, because the coiled coil dimer has much higher vibrational free energy. One reason for the rigidification is that several salt-bridges are formed between the two α-helices. However, in a recent study of the electrostatic contribution of the salt-bridges of the leucine zipper dimer, salt-bridges were found to be thermodynamically stabilizing or destabilizing, depending on the conformational substates and the distance between the pair of the charged groups in the salt-bridges (S. Kumar and R. Nussinov, unpublished results). Thus, our vibrational study of the leucine zipper supports the previous suggestion that an important role of the salt-bridges is to rigidify the protein structure.

We thank Drs. Sandeep Kumar, Neeti Sinha, and, in particular, Jacob V. Maizel for numerous helpful discussions. The research of R. N. and H. Wolfson in Israel has been supported in part by grant number 95–00208 from BSF, Israel, by a grant from the Israel Science Foundation administered by the Israel Academy of Sciences, by the Magnet grant, by the Ministry of Science grant, and by the Tel Aviv University Basic Research grants, and by the Center of Excellence, administered by the Israel Academy of Sciences. This project has been funded in whole or in part with federal funds from the National Cancer Institute, National Institutes of Health, under contract number NO1-CO-56000. The content of this publication does not necessarily reflect the view or policies of the Department of Health and Human Services, nor does mention of trade names, commercial products, or organization imply endorsement by the U.S. government.

REFERENCES

Alm, E., and D. Baker. 1999. Matching theory and experiment in protein folding. *Curr. Opin. Struct. Biol.* 9:189–196.

Baldwin, R. L., and G. D. Rose. 1999a. Is protein folding hierarchic? I. Local structure and peptide folding. *Trends Biochem. Sci.* 24:26–33.

Baldwin, R. L., and G. D. Rose. 1999b. Is protein folding hierarchic? II. Folding intermediates and transition states. *Trends Biochem. Sci.* 24: 77–84.

Bozko, E. M., and C. L. Brooks, III. 1995. First principles calculation of the folding free energy for a three helix bundle protein. *Science.* 269: 393–396.

Elber, R. 1996. Novel mothods for molecular dynamics simulations *Curr. Opin. Struct. Biol.* 6:232–235.

Forman-Kay, J. D. 1999. The 'dynamics' in the thermodynamics of binding. *Nat. Struct. Biol.* 6:1086–1087.

Graziano, G., F. Catanzano, A. Riccio, and G. Barone. 1997. A reassessment of the molecular origin of cold denaturation. *J. Biochem.* 122: 395–401.

Gursky, O., and S. Aleshkov. 2000. Temperature-dependent β-sheet formation in β-amyloid Aβ_{1-40} peptide in water: uncoupling β-sheet folding from aggregation. *Biochim. Biophys. Acta.* 1476:93–102.

Hagler, H. T., P. S. Stern, R. Sharon, J. M. Becker, and F. Naider. 1979. Computer simulation of the conformational properties of oligopeptides: comparison of the theoretical methods and analysis of experimental results. *J. Am. Chem. Soc.* 101:6842–6852.

Haque, T. S., J. C. Little, and S. H. Gellman. 1996. Stereochemical requirements for β-hairpin formation: model studies with four-residue peptides and depsipeptides. *J. Am. Chem. Soc.* 118:6975–6985.

Ibarra-Molero, B., G. I. Makhatadze, and J. M. Sanchez-Ruiz. 1999. Cold denaturation of ubiquitin. *Biochim. Biophys. Acta.* 1429:384–390.

Ishikawa, K., K. Yue, and K. A. Dill. 1999. Predicting the strcutures of 18 peptides using Geocore. *Protein Sci.* 8:716–721.

Kanehisa, M. I., and A. Ikegami. 1977. Structural changes and fluctuations of proteins. II. analysis of the denaturation of globular proteins. *Biophys. Chem.* 6:131–149.

Khechinashvilli, N. N., J. Janin, and F. Rodier. 1995. Thermodynamics of the temperature-induced unfolding of globular proteins. *Protein Sci.* 4:1315–1324.

Kitao, A., S. Hayward, and N. Go. 1998. Energy landscape for a native protein: jumping-among-minima model. *Protein Sci.* 4:1315–1324.

Kumar, S., B. Ma, C. J. Tsai, N. Sinha, and R. Nussinov. 2000a. Folding and Binding Cascades: Dynamic Landscapes and Population Shifts. *Protein Sci.* 9:10–19.

Kumar, S., and R. Nussinov. 2000b. Fluctuation between stabilizing and destabilizing electrostatic contributions of ion pairs in conformers of C-Myc-Max leucine zipper. *Proteins*. In press.

Lacassie, E., A. Delmas, C. Meunier, D. Sy, and Y. Trudelle. 1996. High thermal stability and cold-denaturation of an artificial polypeptide. *Int. J. Pept. Protein Res.* 48:249–258.

Lavigne, P., M. P. Crump, S. M. Gagne, R. S. Hodges, C. M. Kay, and B. D. Sykes. 1998. Insight into the mechanism of heterodimerization from the ^{1}H-NMR solution structure of the c-Myc-Mac heterodimeric leucine zipper. *J. Mol. Biol.* 281:165–181.

Lazaridis, T., and M. Karplus. 1997. "New view" of protein folding reconciled with the old through multiple unfolding simulations. *Science.* 278:1928–1931.

Lee, A. L., S. A. Kinnear, and A. J. Wand. 2000. Redistribution and loss of side chain entropy upon formation of a calmodulin-peptide complex. *Nat. Struct. Biol.* 7:72–77.

Ma, B., and R. Nussinov. 1999. Explicit and implicit water simulations of a β-hairpin peptide *Proteins.* 37:73–87.

Makhatadze, G. I., and P. L. Privalov. 1996. On the entropy of protein folding. *Protein Sci.* 5:507–510.

Maple, J. R., M. J. Hwang, K. J. Jalkanen, T. P. Stockfisch, and A. T. Hagler. 1998. Derivation of class II force fields: V quantum force field for amides, peptides, and related compound. *J. Comput. Chem.* 19: 430–458.

Martins, J. C., W. Zhang, A. Tartar, and M. Lazdunski. 1990. Solution conformation of leiurotoxin I (scyllatoxin) by 1H nuclear magnetic resonance: resonance assignment and secondary structure. *FEBS Lett.* 260:249.

Onuchic, J. N., Z. Luthey-Schulten, and P. G. Wolynes. 1997. Theory of protein folding: the energy landscape perspective. *Annu. Rev. Phys. Chem.* 48:545–600.

Panchenko, A. R., Z. Luthey-Schulten, and P. G. Wolynes. 1996. Foldons, protein structural modules, and exons. *Proc. Natl. Acad. Sci. USA.* 93:2008–2013.

Sturtevant, J. M. 1977. Heat capacity and entropy changes in processes involving proteins. *Proc. Natl. Acad. Sci. USA.* 74:2236–2240.

Tidor, B., and M. Karplus. 1994. The contribution of vibrational entropy to molecular association: the dimerization of insulin. *J. Mol. Biol.* 238: 405–414.

Todd, M. J., and E. Freire. 1999. THe effect of inhibitor binding on the structural stability and cooperativity of the HIV-1 protease. *Proteins.* 36:147–156.

Troyer, J. M., and F. E. Cohen. 1995. Protein conformational landscapes: energy minimization and clustering of a long molecular dynamics trajectory. *Proteins.* 23:97–110.

Tsai, C. J., S. Kumar, B. Ma, and R. Nussinov. 1999a. Folding funnels, binding funnels and protein function. *Protein Sci.* 8:1181–1190.

Tsai, C.-J., and R. Nussinov. 1997. Hydrophobic folding units derived from dissimilar monomer structures and their interactions. *Protein Sci.* 6:24–42.

Tsai, C. J., B. Ma, and R. Nussinov. 1999b. Folding and binding cascades: shifts in energy landscapes. *Proc. Natl. Acad. Sci. USA.* 96:9970–9972.

Viguera, A. R., M. A. Jimenez, M. Rico, and L. Serrano. 1996. Conformational analysis of peptides corresponding to β-hairpins and a β-sheet that represent the entire sequence of the α-spectrin SH3 domain. *J. Mol. Biol.* 255:507–521.

Williams, S., T. P. Causgrove, R. Gilmanshin, K. S. Fang, R. H. Callender, W. H. Woodruff, and R. B. Dyer. 1996. Fast events in protein folding: helix melting and formation in a small peptide. *Biochemistry.* 35: 691–697.

Wintrode, P. L., G. I. Makhatadze, and P. L. Privalov. 1994. Thermodynamics of ubiquitin unfolding. *Proteins.* 18:246–253.

Zidek, L., M. V. Novotny, and M. J. Stone. 1999. Increased protein backbone conformational entropy upon hydrophobic ligand binding. *Nat. Struct. Biol.* 6:1118–1121.